

# Deprotonation of lipid-depleted bacteriorhodopsin

(protein conformation/protonated Schiff base/retinal/cation dependence/pH dependence)

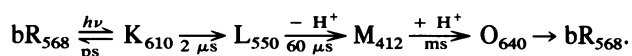
DU-JEON JANG AND M. A. EL-SAYED\*

Department of Chemistry and Biochemistry, University of California, Los Angeles, CA 90024

Contributed by M. A. El-Sayed, May 2, 1988

**ABSTRACT** The removal of 75% of the lipid from bacteriorhodopsin caused the following: (i) decreased efficiency and rate of deprotonation of the protonated Schiff base (as monitored by absorption of the  $M_{412}$  intermediate); (ii) increased efficiency of deprotonation of deionized samples; (iii) a decrease by 1 unit in the pH at which deprotonation ceases; (iv) increased intensity of  $\text{Eu}^{3+}$  emission in  $\text{Eu}^{3+}$ -regenerated deionized delipidated samples; (v) increased exposure of the  $\text{Eu}^{3+}$  sites to water; and (vi) elimination of the dependence of the deprotonation efficiency on the metal cation concentration. These results are discussed in terms of changes in the protein conformation upon delipidation, which in turn control the deprotonation mechanism.

The retinylidene protein bacteriorhodopsin (bR), the other photosynthetic system besides chlorophyll, is one of the protein pigments found in the purple membrane of *Halobacterium halobium* (1, 2). Light-adapted bR contains an all-trans-retinal, which is covalently bound to the protein through a protonated Schiff base (PSB) linkage (1, 3). Upon the absorption of visible light, bR undergoes a photochemical cycle (4) in which the intermediates have lifetimes ranging from picoseconds to milliseconds:



As a result, the PSB is deprotonated during the  $\text{L}_{550} \rightarrow \text{M}_{412}$  transition, leading to a proton-pumping process that increases the proton concentration in the outside surface of the membrane (5). The proton gradient created across the membrane is then used to transform ADP into ATP in the final step of the photosynthesis of bR (6). The understanding of the deprotonation mechanism of the PSB thus becomes very important to our understanding of the molecular mechanism of solar energy storage in nature.

Acidification or removal of cations from bR produces the color transition from the purple form to the blue form (7–12). The blue form of bR is incapable of forming the  $\text{M}_{412}$  intermediate (13), although the isomerization of the retinal and the formation of the  $\text{K}_{610}$  and  $\text{L}_{550}$  intermediates can occur (13, 14). The deprotonation, although it has a nonlinear probability dependence (13, 15) on the metal cation concentration, does not affect the metal ( $\text{Eu}^{3+}$ ) cation binding sites (15). This suggests an indirect (15) involvement of metal cations in the deprotonation process in bR—e.g., by controlling the protein conformational changes during the cycle (16, 17).

Purple membrane contains a variety of diether lipids, amounting to about 25% by weight, that fill the spaces between bR molecules and are all in close contact with the protein (18–21). Most of the lipids are acidic (80%); 70% are phospholipids, mostly the diether analogue of phosphatidylglycerophosphate, and 30% are glycosulfolipids (22, 23).

Szundi and Stoeckenius (24) reported that partially delipidated bR (dLbR) ( $\lambda_{\text{max}} = 561 \text{ nm}$ ) could be reversibly converted to the blue form by acid titration but not by metal cation deionization. They suggested that the purple-to-blue transition is controlled by proton concentration only and that, in native membranes, the cations act only by raising the low surface pH generated by the acidic groups of the lipids.

In this work we study the effect of lipids on the deprotonation process of the PSB in bR by comparing  $\text{M}_{412}$  absorption and the emission from bound  $\text{Eu}^{3+}$  sites in regular bR and dLbR. The results are discussed in terms of changes in the protein conformation upon delipidation.

## MATERIALS AND METHODS

Master slants of the ET1-001 strain of *H. halobium* were kindly supplied to us by W. Stoeckenius and R. Bogomolni (University of California, San Francisco). The bacteria were grown and bR was purified by a combination of procedures (25, 26). bR was delipidated by incubating sample in 20 mM 3-[(3-cholamidopropyl)dimethylammonio]-1-propanesulfonate (CHAPS) (Calbiochem-Behring) containing 5 mM sodium acetate buffer (pH  $\approx 5.4$ ), as described (24). The delipidation process was repeated three times. Excess CHAPS was removed by several washes with water. bR suspensions were deionized according to Kimura *et al.* (10). To avoid complications due to aggregation, bR was incorporated into a 7.5% polyacrylamide gel by the procedure of Mowery *et al.* (9). bR-containing gel slices ( $2 \times 1 \times 0.2 \text{ cm}^3$ ) were placed inside dialysis membrane and deionized by overnight incubation with ion-exchange resin. Before being used for measurements, the bR gel slices were equilibrated overnight in appropriate solutions. The 2-mm-thick bR gel slices in cuvettes were immersed in the same equilibrated solution during measurements.

Steady-state absorption spectra were measured with a Hewlett-Packard 8451 diode-array spectrometer or a Cary 219 UV/visible spectrometer. The kinetics and efficiency of  $\text{M}_{412}$  formation under various conditions were measured by probing the transient absorption of photolyzed bR at 405 nm. The photolysis was accomplished with 570-nm pulses from a  $\text{N}_2$ -pumped dye laser (LN1000 and LN102, Photochemical Research Associates, Oak Ridge, TN) run at a repetition rate of 1 Hz because of the slow decay of  $\text{M}_{412}$  for dLbR. The photolyzing laser pulse had an energy of  $\approx 50 \mu\text{J}$  with a temporal pulse width of  $\approx 0.5 \text{ ns}$  and was focused to  $\approx 2\text{-mm}$  spot size. The probing light from a 100-W Hg arc lamp (model 401, Pek, Sunnyvale, CA) was passed through the sample and filters and focused into a 0.25-m spectrometer (model 82-410, Jarrell-Ash, Waltham, MA). The wavelength-selected probe light was detected by a photomultiplier tube (RCA 1P28A) and recorded with a transient digitizer (model 805, Waveform

The publication costs of this article were defrayed in part by page charge payment. This article must therefore be hereby marked "advertisement" in accordance with 18 U.S.C. §1734 solely to indicate this fact.

Abbreviations: bR, bacteriorhodopsin; dLbR, partially delipidated bR; PSB, protonated Schiff base; CHAPS, 3-[(3-cholamidopropyl)dimethylammonio]-1-propanesulfonate.

\*To whom reprint requests should be addressed.

Recorder, Santa Clara, CA) interfaced to a microcomputer (Apple II+). The signals were averaged for 200–500 shots and then converted to transient absorption in optical density.

The  $\text{Eu}^{3+}$  emission kinetic measurements have been described in detail (27). The  $\text{Eu}^{3+}$ -restored samples were excited at 393 nm (120  $\mu\text{J}$  per pulse,  $\approx 3$ -mm spot size, 10-Hz repetition rate), corresponding to the  $^5\text{L}_6 \leftarrow ^7\text{F}_0$  transition of  $\text{Eu}^{3+}$ . The  $\text{Eu}^{3+}$  emission was collected at  $90^\circ$  to the excitation axis at 625 nm with a 10-nm band width, corresponding to the  $^5\text{D}_0 \rightarrow ^7\text{F}_2$  transition, by using a combination of filters. A gated photomultiplier tube (switched off for 2  $\mu\text{s}$  upon sample excitation) (28) was used for detection and the signal was averaged for 1000–8000 shots. The samples were placed in 3-mm-diameter Teflon tubing. The time constants and preexponential factors for the  $\text{Eu}^{3+}$  emission and  $M_{412}$  absorption kinetics were extracted by using the nonlinear least-squares fitting program CURFIT (29).

## RESULTS

**Delipidation Does Not Affect the Absorption of  $M_{412}$ .** Although delipidation shifts the absorption maximum of bR from 568 to 561 nm, it has no effect on either the extinction coefficient of bR or the absorption maximum of the  $M_{412}$  intermediate. The difference absorption spectrum of dLbR with and without  $M_{412}$  trapping at  $\approx 0^\circ\text{C}$  shows that the absorption maximum of  $M_{412}$  in dLbR is  $\approx 412$  nm as in bR (30). The extinction coefficient of the retinal absorption for bR<sub>568</sub> at  $\lambda_{\text{max}}$  has been found not to change upon the removal of the lipids. Since the  $M_{412}$  absorption does not shift upon delipidation, one would expect that its extinction coefficient also remains unchanged upon delipidation.

**Deprotonation Kinetics of bR and dLbR.** The efficiency of  $M_{412}$  formation for dLbR was compared to that for native bR by using the transient absorbance at 405 nm of dLbR and native bR for the same bR concentration and experimental conditions. The transient absorbance for each sample was normalized by its retinal absorbance at the photolysis wavelength used (570 nm). The observed reduction (by 0.5) of the  $M_{412}$  absorption in dLbR is due to a reduction in the efficiency of  $M_{412}$  formation for bR upon delipidation.

The formation kinetics of  $M_{412}$  for native bR fit well with two rise components as reported earlier (16). Those for dLbR (Fig. 1 Upper) also show fast and slow components but do not fit well with only two rise components, suggesting that the active site(s) in dLbR has a more heterogeneous environment than in bR. The rise times (and the normalized relative amplitudes) are 7.2  $\mu\text{s}$  (0.15) and 57  $\mu\text{s}$  (0.85) for native bR at neutral pH and  $25^\circ\text{C}$  and 18  $\mu\text{s}$  (0.37) and 115  $\mu\text{s}$  (0.63) for dLbR. We notice two significant differences. The formation times of  $M_{412}$  become longer by delipidation. This is consistent with the observed reduced efficiency of  $M_{412}$  formation for dLbR. The second difference is that the relative amplitude of the fast component is increased by delipidation. When we consider that the efficiency of  $M_{412}$  formation is reduced by half, we can notice that the absolute amplitude of the fast component is slightly increased and that of the slow component is greatly decreased by delipidation. Practically, the reduced efficiency of  $M_{412}$  formation for dLbR is due to the reduction of the absolute efficiency of the slow component. According to Hanamoto *et al.* (16), the slow component is dominant under physiological conditions and is the one that is correlated with the proton pump. If the slow one in dLbR is also the one that is correlated with the pump, one might conclude that, if no other complications take place, the pump efficiency could also be reduced by at least a factor of 2 in dLbR.

The decay time of  $M_{412}$  for dLbR (Fig. 1 Lower) is 44 ms at neutral pH and  $25^\circ\text{C}$ . This is much longer than the decay time of 3.9 ms for native bR. The removal or addition of metal

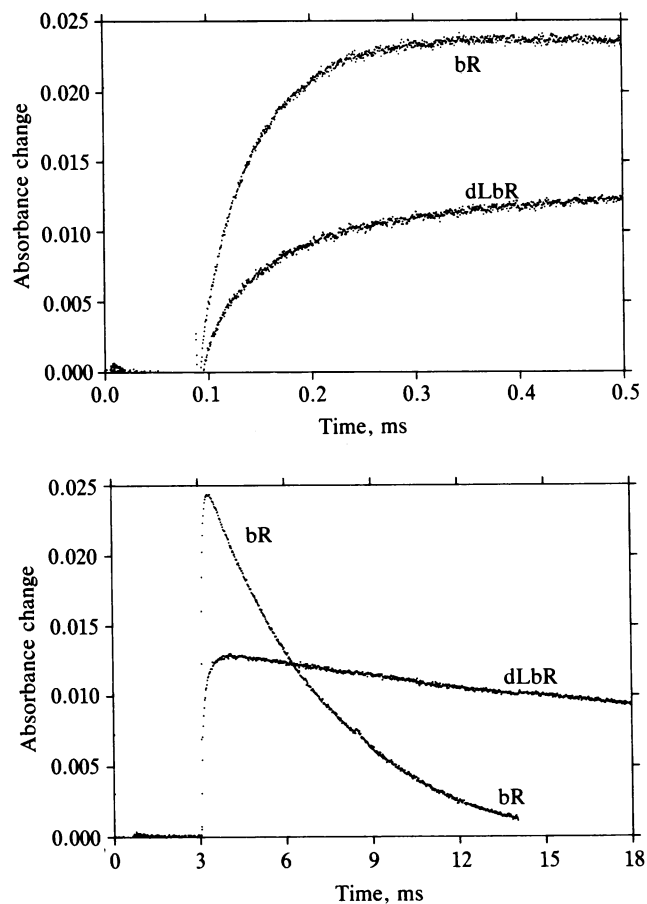


FIG. 1. Comparison of  $M_{412}$  formation (Upper) and decay (Lower) kinetics of dLbR with those of native bR. The kinetics of native bR and dLbR were measured under identical conditions: bR concentration, 22  $\mu\text{M}$ ; temperature,  $25^\circ\text{C}$ ; photolysis wavelength, 570 nm; probe wavelength, 405 nm. These kinetics show an increase in the rise time and a much larger increase in the decay time, suggesting a change in the protein structure around the active site of bR upon delipidation.

cations does not change the formation kinetics, the decay kinetics, or the formation efficiency of  $M_{412}$  in dLbR.

**Lipid Dependence of Deprotonation Probability.** To check the dependence of the deprotonation probability on the degree of delipidation, we measured  $M_{412}$  absorption as a function of CHAPS concentration.  $M_{412}$  absorption was measured for several samples with the same bR concentration, which had been incubated in different CHAPS concentrations overnight. To keep the bR concentration unchanged, the excess CHAPS as well as the dissolved lipid was not removed from these solutions.

Fig. 2 shows the dependence of  $M_{412}$  formation efficiency on CHAPS concentration for native bR in 5 mM sodium acetate buffer solution. Assuming that no, or negligible, change takes place in the absorption spectrum of  $M_{412}$  with the addition of CHAPS, the  $M_{412}$  formation efficiency, calculated from the absorbance change of bR photolyzed at 570 nm and probed at 405 nm, was normalized by the optical density of bR at 570 nm. The delipidation apparently reduces the deprotonation efficiency compared to native bR. The decrease in the  $M_{412}$  formation efficiency of native bR with CHAPS concentration looks similar to the observed decrease in the absorbance at 630 nm of deionized bR (24). The blue form of bR does not form the  $M_{412}$  intermediate (13). However, delipidation enables the deionized bR to deprotonate. The efficiency of  $M_{412}$  formation becomes the same, within experimental errors, for both native and deionized bR

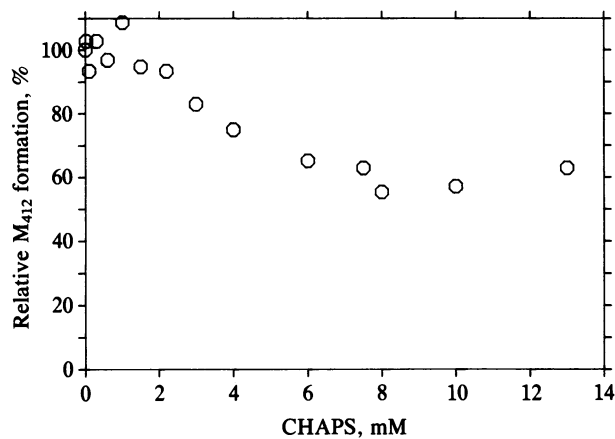


FIG. 2. Efficiency of  $M_{412}$  formation for native bR with various CHAPS concentrations in 5 mM sodium acetate buffer (pH 5.4). Samples with identical bR concentrations were incubated with various concentrations of CHAPS overnight.  $M_{412}$  transient absorption was measured without removal of CHAPS and solubilized lipid. Relative  $M_{412}$  formation efficiencies, calculated from absorbance change of bR excited at 570 nm and probed at 405 nm, were normalized by the optical density of bR at 570 nm.

as CHAPS concentration increases above the critical micelle concentration of  $\approx 8$  mM. This indicates that the  $M_{412}$  formation-efficiency change and the color change, as CHAPS concentration increases, are indeed due to extraction of lipids. Note that the increase of  $M_{412}$  formation with the CHAPS concentration for deionized bR is not due to metal cations contained in the CHAPS solution. CHAPS is a zwitterionic detergent and does not have metal cations as counterions.

**pH Dependence of Deprotonation Probability in dLbR.** Fig. 3 shows the pH dependences of  $M_{412}$  formation efficiency and absorption wavelength for dLbR. For the normalization of the  $M_{412}$  formation efficiency, the change in optical density of bR with pH at the photolyzing wavelength was considered but that of  $M_{412}$  at the probing wavelength with pH was not considered. Since the absorbance rises most sharply near the wavelength of half-maximum absorption, the wavelength shift of dLbR with pH change was recorded as the wavelength at the half-maximum absorbance of the retinal in the red region. As the pH decreases, dLbR changes to the

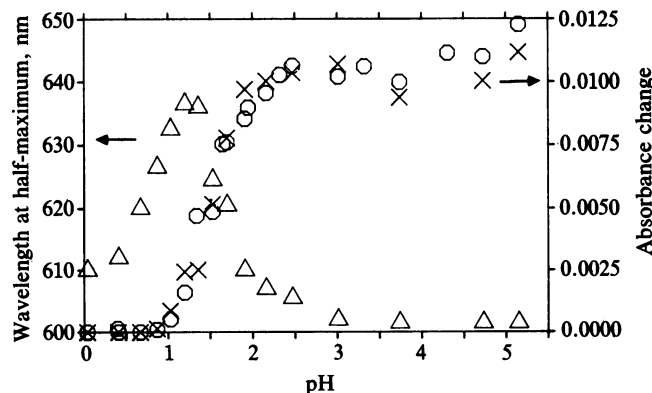


FIG. 3. pH dependence of  $M_{412}$  formation efficiency and absorption wavelength for dLbR in polyacrylamide gel.  $\Delta$ , Wavelength of half-maximum absorbance by retinal in the red region for deionized dLbR;  $\times$ ,  $M_{412}$  formation efficiency for deionized dLbR;  $\circ$ ,  $M_{412}$  formation efficiency for dLbR in 2 mM  $\text{CaCl}_2$ . Relative  $M_{412}$  formation efficiencies, calculated from absorbance change of bR excited at 570 nm and probed at 405 nm, were normalized by the optical density of bR at 570 nm. The left arrow indicates the ordinate label for  $\Delta$  values; the right arrow indicates the ordinate label for  $\circ$  and  $\times$  values.

incomplete acid blue color and then to the acid purple color (Fig. 3,  $\Delta$ ). A similar behavior is seen for the change in the  $M_{412}$  formation efficiency with pH for dLbR ( $\times$ ) and deionized dLbR ( $\circ$ ). For both samples, the efficiency begins to decrease at pH  $\approx 2$  and stops at pH  $\approx 1$  as the pH decreases. The cross point between color change and  $M_{412}$  formation-efficiency change is at pH  $\approx 1.5$  for both dLbR and deionized dLbR. For native bR, this cross point was reported to be at pH  $\approx 2.6$  and to be dependent on the concentration of metal cations (13).

**Nature of  $\text{Eu}^{3+}$  Binding Sites in dLbR.** The  $\text{Eu}^{3+}$  emission intensities for  $\text{Eu}^{3+}$ -regenerated dLbR in  $^1\text{H}_2\text{O}$  and  $^2\text{H}_2\text{O}$  are about 3 times stronger than those for  $\text{Eu}^{3+}$ -regenerated bR with the same  $\text{Eu}^{3+}$  and bR concentrations. The  $\text{Eu}^{3+}$  emission decay from  $\text{Eu}^{3+}$ -regenerated dLbR fits a triexponential decay as does that from  $\text{Eu}^{3+}$ -regenerated bR. The lifetimes and amplitudes obtained from a triphasic  $\text{Eu}^{3+}$  emission-decay fit and the hydration numbers of the  $\text{Eu}^{3+}$ -emitting sites are summarized in Table 1. The largest difference between the decay of dLbR and that of bR is in the relative amplitude of the second component. The emission from this site becomes relatively more intense and seems to have more water coordinations. This suggests that a change in the protein structure takes place as the lipids are removed. For measurements in  $^1\text{H}_2\text{O}$ , the decay constants of the second and third components and all the relative amplitudes change upon delipidation, but in  $^2\text{H}_2\text{O}$  negligible effects on the decay parameters are observed upon delipidation (Table 1).

## DISCUSSION

Several observations suggest that the deprotonation of the PSB (i.e., the formation of  $M_{412}$ ) is controlled by the protein conformational changes during the  $\text{K}_{610} \rightarrow \text{L}_{550} \rightarrow \text{M}_{412}$  process in the cycle. (i) The deprotonation time is  $\approx 60 \mu\text{s}$  (16), which is consistent with the time scale for conformational changes. (ii) A tyrosine dissociates on the same time scale as the deprotonation time of the PSB (32, 33). (iii) The value of the activation energy for both dissociation processes is on the order of hydrogen-bond energies (16). (iv) The time course of quenching of tryptophan fluorescence follows the formation of  $\text{L}_{550}$  and  $\text{M}_{412}$  (34). (v) The deprotonation of the PSB requires more than one metal cation (15), suggesting an indirect involvement like the control of the protein conformational changes. (vi) Native bR, acid or deionized blue bR, and acid purple bR all have different properties. Native bR goes through all the intermediates of the cycle, whereas the acid or deionized blue bR and acid purple bR go through  $\text{K}_{610}$  and  $\text{L}_{550}$  but not through  $\text{M}_{412}$ , suggesting differences in their initial conformations. It was proposed (13) that only native bR has the proper protein conformation that, upon changes from bR to  $\text{L}_{550}$ , could lead to the deprotonation and  $\text{M}_{412}$  formation. Given the above facts, it is of no surprise that partial removal of the lipids, which anchor the protein helices, affects the spatial conformation of the protein. The changes that delipidation produces in the rate of the deprotonation and reprotonation again reflect the change in the protein conformation. The changes in the relative emission intensities and the degree of hydration of the different  $\text{Eu}^{3+}$  sites for  $\text{Eu}^{3+}$ -regenerated deionized dLbR again suggest a change in the protein conformation upon delipidation.

The question arises as to whether there are new binding sites for  $\text{Eu}^{3+}$  in dLbR (as compared to bR) or the same sites but with different degrees of hydration. That the decay constants and the relative amplitudes of bR and dLbR in  $^2\text{H}_2\text{O}$  are almost identical might be explained as follows. In  $^2\text{H}_2\text{O}$ , the observed decay constant is probably all radiative (i.e., the quantum yield of emission in each site is close to unity in  $^2\text{H}_2\text{O}$ ) and is determined solely by the strength of the

Table 1. Lifetimes ( $\tau$ ) and normalized amplitudes of triphasic  $\text{Eu}^{3+}$ -emission decay components and hydration numbers of the  $\text{Eu}^{3+}$  sites for dLbR and bR at room temperature

| Component | In $^1\text{H}_2\text{O}$ |           | In $^2\text{H}_2\text{O}$ |           | $\Delta\tau^{-1}$ ,<br>$\text{ms}^{-1}$ | Water<br>coordination<br>number |
|-----------|---------------------------|-----------|---------------------------|-----------|---|---------------------------------|
|           | $\tau$ , ms               | Amplitude | $\tau$ , ms               | Amplitude |   |                                 |
| dLbR      |                           |           |                           |           |   |                                 |
| 1         | 0.023                     | 0.46      | 0.030                     | 0.64      | 10                                      | 10                              |
| 2         | 0.060                     | 0.43      | 0.15                      | 0.25      | 10                                      | 10                              |
| 3         | 0.22                      | 0.11      | 0.77                      | 0.11      | 3.2                                     | 3                               |
| bR        |                           |           |                           |           |   |                                 |
| 1         | 0.021                     | 0.70      | 0.029                     | 0.70      | 13                                      | 14                              |
| 2         | 0.088                     | 0.24      | 0.18                      | 0.20      | 5.8                                     | 6                               |
| 3         | 0.32                      | 0.06      | 0.79                      | 0.10      | 1.9                                     | 2                               |

$\Delta\tau^{-1}$  is  $\tau^{-1}$  in  $^1\text{H}_2\text{O}$  minus  $\tau^{-1}$  in  $^2\text{H}_2\text{O}$ . The number of coordinated water molecule was calculated by the method of Horrocks and Sudnick (31).

crystal field of the strongly bound protein or lipid groups (e.g., carboxylate or phosphate). That both the relative amplitudes and the decay constants in  $^2\text{H}_2\text{O}$  are the same for bR as for dLbR might then suggest that the binding sites are the same. If so, then these  $\text{Eu}^{3+}$  binding sites are probably protein, rather than lipid, sites. The removal of the lipids opens up the protein structure sufficiently to allow more water to be bound to  $\text{Eu}^{3+}$  in these sites, in particular in the second site. This causes changes in the observed decay constants and relative amplitudes for  $\text{Eu}^{3+}$  in these sites in  $^1\text{H}_2\text{O}$ . It also explains the observation that for bR, two components can fit the observed formation curve of  $M_{412}$ , whereas more components are required for delipidated samples. This suggests an increase in protein heterogeneity when its structure becomes more opened upon delipidation.

The removal of metal cations inhibits the deprotonation steps in bR but not in dLbR. We assume that the CHAPS zwitterion does not bind strongly to the metal cation sites, since exhaustive deionization did not change these observations. A similar observation regarding the color change was made previously (24). It is obvious that both metal cations and lipids control the protein conformation. Thus, the binding of the metal cations changes this conformation so that the protein in the  $L_{550}$  intermediate can assume the conformation required for the deprotonation process to take place. The removal of 75% of the lipid changes the protein conformation in such a manner as to reduce the probability of the deprotonation process by a factor of 2. It remains to be seen whether this reduction occurs at the  $L_{550} \rightarrow M_{412}$  step or at the previous steps in the cycle. It is tempting, however, to suggest that it is during the  $L_{550} \rightarrow M_{412}$  step, as the rate constant of this step is also reduced by a similar factor. If this is true—i.e., if the reduced efficiency is due to the reduction in the rate—there must be another process competing with the deprotonation process, whose rate constant is not greatly affected by the delipidation.

In dLbR, as found in bR (13), the sharp change in the retinal absorption maximum with decreasing pH coincides with the observed decrease in the deprotonation probability. This similarity suggests that the decrease in the pH changes the conformation of the active site of the protein for both bR and dLbR. But since the conformations of these two samples are different, the changes will occur at different pH values. Furthermore, since both retinal absorption and PSB deprotonation reflect properties of the active site, they will respond to the conformational changes of the protein with pH in a similar manner. The effect of pH on the color change (11, 13) or deprotonation (13) in bR has been shown to result from the displacement of the metal cations by protons. If metal cations control the protein conformation in bR (15), their removal could result in conformational changes that lead to color changes and to the inhibition of the deprotonation. Then the  $m\text{H}^+ \rightleftharpoons M^{n+}$  equilibrium (where  $M^{n+}$  is the metal cation)

would control the conformational change. This explained the observed dependence of the transition pH on the metal ion concentration in bR. This is not the case for dLbR, as shown in the color-change studies (24) as well as the present deprotonation studies. In these samples, the removal of the lipid must then have changed the protein conformation around the active site in such a manner as to make it insensitive to the effect of the metal cations. If the mechanism of the deprotonation process in dLbR is the same and is determined by the rate of the protein conformational changes during the  $L_{550} \rightarrow M_{412}$  process (16), then one must conclude that this process is slower in dLbR than in bR. This suggests that the removal of the lipids from bR slows down the protein conformational changes around the active site during the  $L_{550} \rightarrow M_{412}$  process. In addition, delipidation makes the environment of the active site more heterogeneous than in native bR.

How could protein conformational changes control the efficiency of the deprotonation process? To answer this question, one has to understand the mechanism of the deprotonation process itself—i.e., the mechanism of reducing the  $\text{pK}_a$  of the PSB during the photocycle. There have been few proposals in the literature. Retinal isomerization was proposed (35) to reduce the  $\text{pK}_a$  of the PSB. Obviously, this alone cannot account for the sensitivity of the deprotonation of the PSB and a tyrosine to changes in the protein conformation. Furthermore, it was shown that in deionized bR or acid blue bR, isomerization takes place but deprotonation does not. A more recent mechanism (39), which couples isomerization to a change in the counterion (carboxylate) during the cycle, might resolve this difficulty if one proposes that protein conformation could control the location of the second counterion during the cycle. If this is the case, the isomerization alone has to reduce the  $\text{pK}_a$  of the PSB by the full 10–11 units.

As another mechanism, it was proposed (13, 36) that the large change in the  $\text{pK}_a$  of the PSB occurs in steps. The unusually high  $\text{pK}_a$  (=13.3) of the PSB results from an "opsin  $\text{pK}_a$  rise" due to the strong electrostatic interaction with the counterion within the low-dielectric protein medium. The isomerization process reduces the  $\text{pK}_a$  due to the changes in the internal energy of the retinal (35) as well as the increased separation from the counterion (37). This together with changes in the hydrogen-bond geometry around the PSB (38) could lead to a reduction of  $\text{pK}_a$  in the  $L_{550}$  form. During the  $L_{550} \rightarrow M_{412}$  process, the protein conformational changes expose the PSB (and a tyrosine) to a positive field (a positive-to-negative field gradient) that allows the final step in making these species acidic enough to deprotonate in the medium in which they find themselves (to a hydrogen-bonded network or to water channels).

If this mechanism is indeed involved in the deprotonation process, the positive field must be macroscopic rather than

microscopic in nature. It has been shown (14) that metal cations in bR do not interact at very close distances with the PSB during the deprotonation process. The fact that metal cations do not affect the efficiency of the deprotonation process in dLbR supports this conclusion. How can one understand that the removal of metal cations or lipids inhibits the deprotonation process? Furthermore, the recovery of the deprotonation process by deionized bR upon addition of cations (metal or organic) or even anions is nonspecific. The positive-field model could accommodate these observations, since it is the field gradient at the PSB, created during the protein conformational changes in the  $L_{550} \rightarrow M_{412}$  transition, that would result in deprotonation. This field gradient results from the distribution of the positive and negative fields within the protein. This distribution is determined by the number and location of the cations (arginine, lysine, and metal cations), anions (aspartates and glutamates), and dipolar groups and molecules within the protein. Changes in the pH, temperature, or surface charges or other perturbations that might change the protein conformation are expected to change the electric-field gradients within the active site of bR. Changes in the number or position of either cations or anions could lead to changes in the internal field distribution and gradients and could thus affect the deprotonation efficiency. The effect of surface charges in controlling the field gradient around the active site could be either indirect (e.g., by controlling the protein conformation) or direct (if their field penetrates into the region of the active site).

We thank Prof. Walther Stoeckenius for sending us a preprint of ref. 24. We thank Prof. Janos K. Lanyi for careful reading of our manuscript and for useful discussion. This work was supported by the Department of Energy (Office of Basic Energy Sciences) under Grant DE-FG03-88ER13828.

1. Oesterhelt, D. & Stoeckenius, W. (1971) *Nature (London) New Biol.* **233**, 149–152.
2. Stoeckenius, W. & Bogomolni, R. A. (1982) *Annu. Rev. Biochem.* **52**, 587–619.
3. Bridgen, J. & Walker, I. D. (1976) *Biochemistry* **15**, 792–798.
4. Lozier, R., Bogomolni, R. A. & Stoeckenius, W. (1975) *Biophys. J.* **15**, 955–962.
5. Dencher, N. & Wilms, M. (1975) *Biophys. Struct. Mech.* **1**, 259–271.
6. Belliveau, J. W. & Lanyi, J. (1977) *Arch. Biochem. Biophys.* **178**, 308–314.
7. Moore, T. A., Edgerton, M. E., Parr, G., Greenwood, C. & Perham, R. N. (1978) *Biochem. J.* **171**, 469–476.
8. Tokunaga, F. & Ebrey, T. (1978) *Biochemistry* **17**, 1915–1922.
9. Mowery, P. C., Lozier, R. H., Chae, Q., Tseng, Y.-W., Taylor, M. & Stoeckenius, W. (1979) *Biochemistry* **18**, 4100–4107.
10. Kimura, Y., Ikegami, A. & Stoeckenius, W. (1984) *Photochem. Photobiol.* **40**, 641–646.
11. Chang, C.-H., Chen, J.-G., Govindjee, R. & Ebrey, T. (1985) *Proc. Natl. Acad. Sci. USA* **82**, 396–400.
12. Ariki, M. & Lanyi, J. K. (1986) *J. Biol. Chem.* **261**, 8167–8174.
13. Chronister, E. L., Corcoran, T. C., Song, L. & El-Sayed, M. A. (1986) *Proc. Natl. Acad. Sci. USA* **83**, 8580–8584.
14. Kobayashi, T., Ohtani, H., Iwai, J., Ikegami, A. & Uchiki, H. (1983) *FEBS Lett.* **162**, 197–200.
15. Corcoran, T. C., Ismail, K. Z. & El-Sayed, M. A. (1987) *Proc. Natl. Acad. Sci. USA* **84**, 4094–4098.
16. Hanamoto, J. H., Dupis, P. & El-Sayed, M. A. (1984) *Proc. Natl. Acad. Sci. USA* **81**, 7083–7087.
17. Dupis, P., Corcoran, T. C. & El-Sayed, M. A. (1985) *Proc. Natl. Acad. Sci. USA* **82**, 3662–3664.
18. Blaurock, A. E. & Stoeckenius, W. (1971) *Nature (London) New Biol.* **233**, 152–155.
19. Henderson, R. & Unwin, P. N. T. (1975) *Nature (London)* **257**, 28–32.
20. Jost, P. C., McMillen, P. A., Morgan, W. D. & Stoeckenius, W. (1978) in *Light Transducing Membranes: Structure, Function, and Evolution*, ed. Deamer, P. W. (Academic, New York), pp. 141–155.
21. Glaeser, R. M., Jubb, J. S. & Henderson, R. (1985) *Biophys. J.* **48**, 775–780.
22. Kushwaha, S. C., Kates, M. & Martin, W. G. (1975) *Can. J. Biochem.* **53**, 284–292.
23. Kates, M., Kushwaha, S. C. & Sprott, G. D. (1982) *Methods Enzymol.* **88**, 98–105.
24. Szundi, I. & Stoeckenius, W. (1987) *Proc. Natl. Acad. Sci. USA* **84**, 3681–3684.
25. Oesterhelt, D. & Stoeckenius, W. (1974) *Methods Enzymol.* **31**, 667–678.
26. Becher, B. M. & Cassim, J. Y. (1975) *Prep. Biochem.* **5**, 161–178.
27. Corcoran, T. C. (1987) Dissertation (Univ. of California, Los Angeles), pp. 69–82.
28. Hopewell, W. D. (1980) Dissertation (Univ. of California, Los Angeles), pp. 36–42.
29. Bevington, P. R. (1967) *Data Reduction for the Physical Science* (McGraw-Hill, New York), pp. 237–240.
30. Oesterhelt, D. & Hess, D. (1973) *Eur. J. Biochem.* **37**, 316–326.
31. Horrocks, W. DeW., Jr., & Sudnick, D. R. (1981) *Acc. Chem. Res.* **14**, 384–392.
32. Hess, B. & Kuschmitz, D. (1979) *FEBS Lett.* **100**, 334–340.
33. Ottolenghi, M. (1980) *Adv. Photochem.* **12**, 97–200.
34. Fukumoto, J. M., Hopewell, W. D., Karvaly, B. & El-Sayed, M. A. (1981) *Proc. Natl. Acad. Sci. USA* **78**, 252–255.
35. Schulten, K. & Tavan, P. (1978) *Nature (London)* **272**, 85–86.
36. Chronister, E. L. & El-Sayed, M. A. (1987) *Photochem. Photobiol.* **45**, 507–513.
37. Warshel, A. (1979) *Photochem. Photobiol.* **30**, 285–290.
38. Schneiner, S. & Hillenbrand, E. (1985) *Proc. Natl. Acad. Sci. USA* **82**, 2741–2745.
39. Engelhard, M., Gerwert, K., Hess, B., Kreutz, W. & Siebert, F. (1985) *Biochemistry* **24**, 400–407.